Capacity-based optimization using whale optimization technique of a power distribution network

Simachew, Bawoke; Khan, Baseem; Guerrero, Josep M.; Padmanaban, Sanjeevikumar; Mahela, Om Prakash; Alhelou, Hassan Haes

Published in:
Engineering Reports

DOI (link to publication from Publisher):
10.1002/eng2.12455

Publication date:
2022

Document Version
Publisher's PDF, also known as Version of record

Received: 4 December 2020 | Revised: 31 July 2021 | Accepted: 24 August 2021

DOI: 10.1002/eng2.12455

RESEARCH ARTICLE

Engineering Reports Open Access WILEY

Capacity-based optimization using whale optimization technique of a power distribution network

Bawoke Simachew[1] | Baseem Khan[2] | Josep M. Guerrero[3] | Sanjeevikumar Padmanaban[4] | Om Prakash Mahela[5] | Hassan Haes Alhelou[6]

[1]Department of Electrical Engineering, National Taipei University of Technology, Taipei, Taiwan

[2]Department of Electrical and Computer Engineering, Hawassa University, Awasa, Ethiopia

[3]Center for Research on Microgrids – CROM, Aalborg University, Aalborg, Denmark

[4]CTiF Global Capsule, Department of Business Development and Technology, Aarhus University, Herning, Denmark

[5]Power System Planning Division, Rajasthan Rajya Vidyut Prasaran Nigam Ltd., Jaipur, India

[6]Department of Electrical Power Engineering, Tishreen University, Lattakia, Syria

Correspondence
Baseem Khan, Department of Electrical and Computer Engineering, Hawassa University, Awasa, Ethiopia.
Email: baseem.khan04@gmail.com

Funding information
Villum Fonden, Grant/Award Number: 25920

Abstract

In the power distribution network, real power loss and voltage profile management are critical issues. By providing active and reactive power support, both of these issues can be managed. Distributed generation (DG) and capacitor bank (QG) can be utilized to solve these issues. Therefore, this paper utilized optimally placed and sized DG and capacitor (QG) to minimize losses and improve the voltage profile. The overall problem is optimized using an upgraded method of the fitness assignment and solution chasing based on the aggregate approach called multi-objective whale optimization algorithm (MWOA). Wind and solar photovoltaic sources with biomass are utilized as the DG sources with their probabilistic outputs. The developed method is tested using two practical feeders of Bahir Dar city distribution network, Ethiopia. The results of loss minimization and voltage profile enhancement with MWOA are compared with multi-objective particle swam optimization (MPSO) with an equal number of iterations to show the superiority of the developed method.

KEYWORDS

capacitor placement, distributed generation, loss minimization, particle swarm optimization, whale optimization algorithm

JEL CLASSIFICATION

Electrical and electronic engineering

1 | INTRODUCTION

In distribution system, voltage is stepped down; as a result, system loss is higher. According to the Electric Power Research Institute (EPRI),[1,2] the distribution loss is about 70% of all energy loss and it is even higher during peak load conditions. Various researchers indicate that the distribution system has more than 13% losses of the total energy production. Therefore, the distribution loss minimization is the major issue in the smart grid system. Various techniques are utilized by researches to mitigate these issues such. Optimal placement of the distributed generation (DG) sources is one of the effective techniques utilized to minimize the distribution system losses with voltage profile improvement. DG sources incorporated solar photovoltaic (SPV) system, wind turbines, micro turbines, biomass, and so forth. For selecting the

type of DG sources, site selection and resource assessment are performed. Further feasibility analyses of the selected DG sources are performed for the better utilization of these sources. Optimal placement and sizing of DG sources are the critical issues in the smart power system as these will critically minimized the system losses as well enhanced the voltage profile of the system. Different optimization techniques are utilized by the various researchers to optimally place and size the DG sources. Further, load flow techniques are required to generate the input data for the optimal placement of DG sources. Recent improved load flow techniques[3,4] can be utilized to obtain input data for performing the optimal placement problem of DG sources.

1.1 | Related work

For a decade various power flow techniques with different optimization methods are utilized to perform the optimal placement and sizing of the DG sources in the power system. From these recent technologies, some of them are critically reviewed. In Reference 5, Ali et al. used mixed-integer linear programming optimization technique to size and place the battery-coupled distributed photovoltaic generators along with genetic algorithm. In Reference 6, Lalitha et al. applied symbiotic organisms search technique to find and locate the DG and QG optimally. In Reference 7, Abdelaziz et al. used flower pollination optimization technique and power loss index for the capacitor optimal location and sizing and to reduce the overall cost and power loss. In Reference 8, Reddy et al. used WOA for the optimal sizing of renewable energy resources. In Reference 9, Wang et al. used particle swam optimization (PSO) for the reactive power optimization and sizing of the capacitor in radial distribution feeders. In Reference 10, Bhullar et al. used artificial bee colony (ABC) and cuckoo search hybrid technique for optimal integration of multi-distributed production. In Reference 11, Xie et al. presented reactive power optimization for distribution networks based on distributed random gradient-free algorithm. In Reference 12, Boktor et al. proposed optimal distribution power flow including shunt capacitor allocation. In Reference 13, Elsheikh et al. proposed optimal capacitor placement and sizing for radial electric power systems. In Reference 14, Thang and Minh proposed optimal allocation and sizing of capacitors for distribution systems reinforcement. In Reference 15, Hassanzadeh Farda et al. used PSO for sizing and placement of the renewable energy-based DG units in distribution systems by considering load growth. In Reference 16, Prakash et al. proposed an optimal siting of capacitors in the radial distribution system using WOA. In Reference 17, Kumar et al. proposed an optimal placement and sizing of renewable DGs and capacitor banks for radial distribution networks. In Reference 18, the same authors developed multi-objective PSO based optimal placement of solar power DG in radial distribution network. In Reference 19, Shehata et al. used improved whale optimization algorithm to optimal place capacitor banks to get maximum save for power loss and successful in reducing the loss without violating the constrained limits. In Reference 20, Ang et al. utilized multi-objective whale optimization algorithm (MWOA) for real power loss and bus voltage deviation (VD) minimizations of grid connected micro power system with non-firm small power plants. Voltage magnitude of transformer taps changers are utilized as control variables and successfully executed optimal power flow. In Reference 21, Al-Ammar et al. utilized the ABC technique to solve the optimal sizing and siting problem of DG sources. In Reference 22, Roy and Das performed the optimal allocation of both active and reactive DG sources in a droop controlled isolated microgrid system. In Reference 23, Ziad et al. proposed DG sources planning and placement by utilizing graphically dependent network configuration and Archimedes optimization technique, respectively. In Reference 24, Öner and Abur performed optima placement of DG sources against extreme events utilized the voltage stability constraints. In Reference 25, Rafi and Dhal utilized the hybrid optimization algorithm for the optimal placement of the DG sources with reorganization. In Reference 26, Ahmadi et al. performed optimum coordination of centralized and distributed renewable power generation incorporating battery storage system into the electric distribution network by utilizing multi-objective multi-verse optimization (MOMVO). In Reference 27, Tolabi et al. utilized a novel optimization algorithm, that is, thief and police algorithm for the optimal reconfiguration and placement of the capacitor and DG sources. In Reference 28, Routray et al. used the wake analysis for wind power production to minimize losses in the distribution network.

1.2 | Research gap

After detailed and critically analyzed the various research, different techniques are missing to incorporate the following issues:

- Various literatures did not utilize the practical system implementation of the proposed work.
- Different research missed a detailed cost analysis in terms of the DG sources incorporation cost.
- Much literature did not use the total feeders' carrying capacity as a constraint to get the least power loss

1.3 | Contribution of the work

This work performed the placement of the DG and capacitors (QG) units to support the unbalanced reactive power and for the maximum active power loss reduction. Therefore, this study presented the total real power loss reduction with voltage profile improvement of the two critical practical feeders of the Bahir Dar distribution network by optimally quantifying and locating the DG and capacitors (QG). So, this work incorporated the practical network to find possible minimum power loss by considering the maximum network capacity limits (upper limit constraint). To perform this research, a recent and powerful optimization technique called whale optimization algorithm (WOA)[29] is used as it has a fast convergence, large input carrying capacity and multi direction searching capability.

Incorrect size of DG and QG may increase the system losses as compared to the base case condition. WOA is utilized for the proper site and size of the DG. Further, it is applied to locate and size of the capacitors. Therefore, in this work, MWOA is used for optimal sizing and siting of DG and QG. Hence, this work used a mechanism called feeder carrying capacity limit under the constraint condition for distribution network optimization. It is mentioned that DG and QG size can be less than the total power required by the system. Therefore, for the purpose of network security, in this work, 80% of the total power demand is taken as the upper limit of DG and QG. The significant contributions of this work are as follows:

- Two practical feeders of the Bahir Dar distribution network are considered and modeled to know the performance of the real system.
- Multi-objective WOA is utilized to perform the optimal placement and sizing of the DG and QG sources in the system.
- Actual local metrological solar irradiation and wind speed data are considered to assess the energy outputs from the DG sources.
- Total feeders' carrying capacity is considered as limits to get the maximum possible least power loss. It is optimally quantifying and locating the DG and QG within the network carrying capacity limit and a way of searching the possible minimum loss from the all buses instead of searching the relative weakest bus. Here the maximum size or upper limit of DG/QG will be decided from the limit of network carrying capacity and the program will keep the performance.
- A detailed comparative analysis of the developed MWOA method is performed using multi-objective particle swam optimization (MPSO),[30] which shows the superiority of the MWOA.

1.4 | Organization

The paper is organized as follows: Section 2 discussed the background of the performed research. Section 3 presented methodology and problem formulation. Section 4 presented the results and comparative analysis, followed by the conclusion.

2 | BACKGROUND

This section discussed the background of the study area, with selection and assessment of the DG and reactive power supply sources for the study area is presented in this section.

2.1 | SPV system

This work used the SPV system to generate active power as DG source.

2.1.1 | Power output of PV array

The out power of photo voltaic (PV) array is presented as[31,32]

$$P_{pv} = A_C \eta_{MP} \eta_E G_T \tag{1}$$

where, P_{pv} represents the output of PV array, A_C is the array area, η_{MP} is the maximum power point efficiency of the array (≈14%), η_E is the efficiency of power-conditioning equipment (≈90%), and G_T is the incident solar radiation on the array.

2.1.2 | Solar radiation estimations

Solar declination angle (δ) is the angle between the earth's equatorial plane and the earth sun line. The solar hour angle ω is the angle Earth has rotated since solar noon. The relation between these angles is given by[31,32]:

$$\delta = 23.45 sin\left(360 \frac{284 + n_d}{365}\right) \tag{2}$$

where, δ represents solar declination angle (°), n_d is day number of the year starting at January 1st as 1, ω is ($t_s - 12$ h). $15^{\circ}/h_r$, t_s is the solar time in hour, ω is a solar hour angle (°). The value of $t_s$is 12 h at solar noon and 13.5 h 90 min later.[31,32]

$$sin(\alpha) = sin(\phi) sin(\delta) + cos(\phi) cos(\delta) cos(\omega) \tag{3}$$

where, α_s represents the solar altitude (°) and ϕ is latitude (°).[31,32]

$$sin(\gamma_s) = \left[\frac{cos(\delta) sin(\omega)}{cos(\alpha_s)}\right] \tag{4}$$

where, γ_s represents the solar azimuz (°). The sunset/sunrise angle is given by[31,32]

$$\omega_s = cos^{-1}(-tan\phi tan\delta) \tag{5}$$

The solar angle of incident θ_i is the angle between the solar beam and normal to the solar panel, which is given by:

$$cos(\theta_i) = [sin\delta sin\phi cos\beta - sin\delta cos\phi sin\beta cos\gamma + cos\delta cos\phi cos\beta cos\omega + sin\phi sin\beta cos\gamma cos\omega + cos\delta sin\beta sin\gamma sin\omega] \tag{6}$$

The solar constant (G_{sc}) is equals to1367 W/m^2. The extraterrestrial irradiance on a surface at normal incidence (G_{on}) can be expressed as[31,32]:

$$G_{on} = G_{sc}\left[1 + 0.033 cos\frac{2\pi n_d}{365}\right] \tag{7}$$

The extraterrestrial irradiance incident on a horizontal plane at an arbitrary angle of incidence is expressed as.[33]

$$G_o = G_{on} cos(\theta_z) \tag{8}$$

where, θ_z is the zenith angle between the solar beam and the vertical. θ_z and θ are not in the same plane.

Integrating the solar constant (extraterrestrial irradiance) over the day length gives us daily solar radiation on the horizontal surface.[31,32]

$$H_o = \left(\frac{24 \times 3600}{\pi}\right) G_{sc}\left[\left(1 + 0.033 cos\left(\frac{360 n_d}{365}\right)\right) \times \left(cos\phi cos\delta sin\omega_s + \frac{2\Pi}{360}\omega_s sin\phi sin\delta\right)\right] \tag{9}$$

where, δ is declination angle (°),and ω_s is sunset hour angle (°). For Bahir Dar city the computed solar irradiance is as follows:

$$Ho = 1367 * [(1 + 0.033 * \cos\left(\frac{360 * 181.42}{365}\right) * \left(\cos 11 * \cos(-0.752) * \sin\left(89.99 + \frac{2\pi}{360} * 89.99 \sin 11 \sin(-0.752\ )\right)\right] = \frac{1322.73\ \mathrm{W}}{\mathrm{m}^2}.$$

2.1.3 | Solar energy resource in Bahir Dar

Bahir Dar is located near the equator; its solar resource is of significant potential. The annual average daily radiation in Bahir Dar reaching the ground is estimated to be 6 kWh/m^2/day, which varies from a minimum of 5.26 kWh/m^2/day in July to a maximum value of 6.86 kWh/m^2/day in February.[34] An indirect estimation of solar radiation is performed by ground level measurement. Table 1 presented the estimated monthly solar radiation for Bahir Dar district.

For the renewable hybrid power system design of Bahir Dar, the estimated monthly average global solar radiation from the ground measured sunshine hour data from National Meteorological Service Agency, Ethiopia summarized and listed in Table 2 and uses for the feasibility study of the proposed hybrid renewable energy system using HOMER.

2.2 | Wind turbine

The second distributed energy source used in this work is the wind turbine.

2.2.1 | Speed and power relations

The kinetic energy of wind in joules is presented by[31]:

$$\text{Kinetic Energy} = \frac{1}{2}mV^2 \tag{10}$$

where, m represents mass, V is the wind speed.

TABLE 1 Estimated monthly solar radiation for Bahir Dar district (Lat = 11.4)

Mid of month	N_d	δ (°)	ω_s (°)	N (h)	n	n/N	Ho (kW/m^2/d)	NMSA (kW/m^2/d)	NASA (kWh/m^2/d)	SWERAREL (kWh/m^2/d)
Jan	15	−21.270	87.326	11.644	9.78	0.84	9.25	6.40	6.27	6.335
Feb	45	−13.620	88.336	11.778	9.85	0.836	9.85	6.79	6.86	6.885
Mar	74	−2.819	89.662	11.955	9.56	0.8	10.36	6.98	6.78	7.072
Apr	105	9.415	91.138	12.152	8.91	0.733	10.47	6.76	6.01	6.491
May	135	18.792	92.337	12.312	7.23	0.587	10.22	5.95	5.78	6.089
Jun	166	23.314	92.960	12.395	6.83	0.551	9.22	5.66	5.35	5.867
Jul	196	21.517	92.708	12.361	5.87	0.475	9.98	5.36	5.26	5.392
Aug	227	13.784	91.685	12.225	6.79	0.555	10.04	5.85	5.91	6.122
Sep	258	2.217	90.266	12.035	8.35	0.694	10.29	6.50	6.29	6.68
Oct	288	−9.599	88.839	11.845	7.83	0.661	10.34	6.13	5.39	6.108
Nov	319	−19.148	87.616	11.682	8.57	0.734	9.98	6.05	5.69	6.258
Dec	349	−23.335	87.037	11.605	9.56	0.824	9.38	6.18	6.01	6.138
Avg	181.4	−0.752	89.99				9.04	6.218	5.96	6.286

TABLE 2 Monthly average solar radiation

Month	Clearances Index	Daily radiation (kWh/m²/d)
January	0.724	6.335
February	0.728	6.885
March	0.695	7.072
April	0.616	6.491
May	0.581	6.089
June	0.566	5.867
July	0.519	5.392
August	0.586	6.122
September	0.652	6.680
October	0.634	6.108
November	0.705	6.258
December	0.723	6.281
Average	0.640	6.281
Annual average (kWh/m²/d)		

The power generated in watts is given by[31]:

$$\text{Power} = \frac{1}{2}(\text{Mass Flow per Second})V^2 \tag{11}$$

where, P represents mechanical power in the moving air (watts), ρ is air density (kg/m^3), A is area swept by the rotor blades (m^2), and V represents the velocity of the air (m/s).

The mechanical power output from the upstream wind is presented by,

$$P = \frac{1}{2}(\rho AV)V^2 = \frac{1}{2}\rho AV^3 \tag{12}$$

where, AV represents the volumetric flow rate, and ρAV represents the mass flow rate of the air in kilograms per second. The power density of the selected area is used to compare two potential wind sites in watts per square meter and presented by:

$$\text{Specific Power of Site} = \frac{1}{2}\rho V^3 \tag{13}$$

2.2.2 | Wind speed distribution

The mean wind velocity is given by,

$$V_{av} = \int_0^\infty vf(v)dv \tag{14}$$

The variation in wind speed is the best described by Weibull probability distribution function f with two parameters, the shape parameter k, and the scale parameter c. The following equation gives the probability of wind speed being v during any time interval[31]:

$$f(u) = \left(\frac{k}{c}\right)\left(\frac{u}{c}\right)^{(k-1)} e^{-\left(\frac{u}{c}\right)^k} \text{ for } 0 < u < \infty, k > 1, c > 0 \tag{15}$$

The cumulative distribution $F(u)$ is given by,

$$F(u) = 1 - e^{\left(\frac{u}{c}\right)^k} \tag{16}$$

where, u is the wind speed, $k(>0)$ is the shape parameter, and $c(>0)$ is the scale parameter of the distribution. The value of the shape factor is varying from 1 to 4.

$$V_{ave} = \Gamma\left(1 + \frac{1}{k}\right) \tag{17}$$

$$\Gamma(x) = \int_0^\infty \xi^{x-1} exp(-\xi) d\xi \text{ and } \Gamma(x) = \Gamma(x+1) = x\Gamma(x) \tag{18}$$

For $k = 2$;

$$C = \frac{2}{\sqrt{\pi}} V_{ave} \tag{19}$$

Average wind speed and scale factor in the equation are used to find the probability distribution using HOMER software.

The annual average wind speed for that hour is represented by each of the 24 values of the average diurnal profile.[31]

$$v_i = \bar{v}\left\{1 + \delta cos\left[\left(\frac{2\pi}{24}\right)(i - \phi)\right]\right\} \tag{20}$$

2.2.3 | Wind power density distributions and mean power density

The average power density is given by[31]:

$$P_{wm} = \frac{1}{2}\rho C^3 \Gamma\left(1 + \frac{3}{k}\right) \tag{21}$$

$$V_{ave} = C\Gamma\left(1 + \frac{1}{k}\right) \tag{22}$$

Γ is the gamma function and given as:

$$for\ k = 2\ and\ \Gamma\left(1 + \frac{3}{2}\right) = \frac{3}{2} * \frac{\sqrt{\pi}}{2} = 3\frac{\sqrt{\pi}}{4} \tag{23}$$

The air density varies with altitude and therefore the formula that governs is

$$\rho = \rho_o e^{-\left(\frac{0.297 H_m}{3048}\right)} or\ \rho = \rho_o - 1.194 * 10^{-4} H_m \tag{24}$$

Finally, power density for each month is given by:

$$P_{wm} = \frac{1}{2}\rho C^3 \frac{3\sqrt{\pi}}{4} \tag{25}$$

The wind power density values for each month for Bahir Dar city are calculated and listed in Table 3 below, where ρ equals to 1.225 kg/m^3.

The energy density characteristics at a height of 50 m are presented in Table 4 below.

TABLE 3 Monthly wind power density

Month	Bahir Dar city with $k = 2$		
	Monthly avg. wind speeds (m/s)	Scale factor	Power density (W/m^2) [Elev. = 78 m]
January	10.1	11.4519	1222.9
February	10.1	11.3535	1191.6
March	10.1	11.3706	1197
April	10.2	11.4745	1230.1
May	10.0	11.3070	1177
June	10.0	11.2623	1163.1
July	10.0	11.3396	1187.2
August	10.2	11.4853	1233.6
September	10.1	11.3492	1190.2
October	10.2	11.4870	1234.1
November	10.1	11.4345	1217.3
December	10.1	11.3606	1193.8
Monthly annual avg.	10.1	11.3897	1203

TABLE 4 Wind energy output category benchmark[31]

Wind resource category	Wind level	Wind power density (W/m^2)	Wind speed at 50 m (m/s)
Poor	1	50–200	3.5–5.6
Marginal	2	200–300	5.6–6.4
Moderate	3	300–400	6.4–7.0
Good	4	400–500	7.0–7.5
Excellent	5	500–600	7.5–8
Excellent	6	600–800	8–8.8
Excellent	7	Above 800	Above 8.8
The total area covered by marginal to excellent wind regions			

TABLE 5 Technical data for Vestas V82 wind turbine manufacturers' data sheet

Specification for VESTAS V82 wind turbine	
Available towers	59/70/78
Rotor	82 m diameter, 5.281 m^2 swept area, 14.4 rpm
Cut-in wind speed	3.5 m/s
High wind speed	20 m/s
Rated power wind speed	1.65 MW at 13 m/s

Observing Table 4, the power density category of Bahir Dar city is on the seventh category, which indicates the region, has great potential for electric power generation. The technical data of Vestas V82 wind turbine according to the manufacturer data sheet are presented in Table 5.[33]

2.2.4 | Wind speed–height correction

The average wind speed increases with the height is approximately 1/7th of the power for the ideal smooth plane.[31]

$$\frac{v(z_2)}{v(z_1)} = \left(\frac{z_2}{z_1}\right)^{\alpha} \tag{26}$$

where, $V(z_2)$ is the wind speed at the desired height of z_2; $v(z_1)$ is the wind speed measured at a known height z_1, and α is a coefficient known as the wind shear exponent. A modified formula is best suited for estimating the wind speed at hub height.

$$\frac{v(z_{hub})}{v(z_{anem})} = \frac{ln\left(z_{hub}/z_o\right)}{ln\left(z_{anem}/z_o\right)} \tag{27}$$

2.2.5 | Wind power generation

As the power generated for wind turbine is given by,

$$P = \frac{1}{2}\rho A V^3 \tag{28}$$

The air density ratio is provided by,

$$\frac{\rho}{\rho_o} = \left(1 - \frac{BZ}{T_o}\right)^{g/RB}\left(\frac{T_o}{T_o - BZ}\right) \tag{29}$$

The air density under standard conditions, that is, at sea level and 15°C is 1.22 kg/m^3. The hourly generation from wind turbine is given by,

$$\begin{cases} P_e = 0 & (u < u_c) \\ P_e = a + bu^k & (u_c \le u \le u_R) \\ P_e = P_{eR} & (u_R \le u \le u_f) \\ P_e = 0 & (u > u_f) \end{cases} \tag{30}$$

The coefficients a and b is given by:

$$a = \frac{P_{eR}u_{eR}^k}{u_c^k - u_R^k} \text{ and } b = \frac{P_{eR}}{u_R^k - u_c^k}$$

2.2.6 | Annual wind energy production and capacity factor

The capacity factor of wind turbine is given as[31]:

$$C_F = \left\{\frac{exp\left[-\left(\frac{u_c}{c}\right)^k\right] - exp\left[-\left(\frac{u_R}{c}\right)^k\right]}{\left(\frac{u_R}{c}\right)^k - \left(\frac{u_c}{c}\right)} - exp\left[-\left(\frac{u_F}{c}\right)^k\right]\right\} \tag{31}$$

By using $U_c = 3$ m/s, $U_R = 13$ m/s, $U_F = 20$ m/s, and $C = 10.43$ m/s, the computed value of the capacity factor is 0.466. Therefore, the annual energy production of a single wind turbine is 6,602,587.2 kWh by taking nominal rated power as 1650 kW.[31]

The minimum output power from the cut in speed (i.e., 3 m/s) is 26.27 kW power. The estimated capacity factor and annual energy production from a single Vestas V82 wind turbine are summarized in Table 6.

The estimated capacity factor indicates that all values and annual energy production are within the acceptable range from a single Vestas V82 wind turbine.

TABLE 6 V82 wind turbine-estimated capacity factor and annual energy production[31]

District	Scale factor (C)	V_{av}	K	CF (capacity factor)	E (GWh)
BDR	11.3897	10.1	2	0.47	6.602587

2.3 | Biomass energy

The third distributed energy source used in this work is the biomass energy source as it is widely available in Bahir Dar, Ethiopia. Bahir Dar is located in the northwest of Ethiopia, where most of the country's agricultural crops are cultivated. Apart from huge availability of Corn, beans, teff, barley and wheat in Gojjam and Gonder cities, which are near Bahir Dar, the forest around the city, municipal solid waste, biosolids, industrial waste, animal manures, forestry residual, landscaping and tree clipping can be used as biomass resources. Figure 1 presents the Crop residue biomass resource in Gojjam, Bahir Dar, Ethiopia.

Table 7 presented the Crop cultivation areas in the parts of Amhara region, near Bahir Dar, Ethiopia.

2.3.1 | Physical properties of biomass

The content of moisture is estimated on the basis of dry and wet.[35,36] On the wet basis, moisture content is calculated as follows:

$$MC_W = \frac{\text{mass of water}}{\text{mass of wet biomass}} = h_{wet} = \frac{m_{tot} - m_{dry}}{m_{tot}} \times 100\% \tag{32}$$

FIGURE 1 Crop residue biomass resource in Gojjam

TABLE 7 Crop cultivation areas in some parts of Amhara region near Bahir Dar[35,36]

District	Total area (h)
Yilmama Densa	99, 180
Quarit	61, 473
Gozamin	121, 807
Sinan	38, 640
Farta	107, 077
Lai-gaint	154, 866
Banja	45, 618
Guagusa-shikudad	30, 432
Awi-zone	271, 000
Sum	930, 093

Further, the estimation of the moisture content on the dry basis is calculated as,

$$MC_D = \frac{\text{mass of water}}{\text{mass of dry wood}} = h_{dry} = \frac{m_{tot} - m_{dry}}{m_{dry}} \times 100\% \tag{33}$$

where, m_{tot} represents the total mass, including moisture, m_{dry} represents the mass of the dry substance, and $m_{tot} - m_{dry}$ represents the moisture mass.

2.3.2 | Heat balance in a complete combustion

Generally, the heat generated from combustion is equal to the heat required for vaporizing the available water plus heat related to vaporize water mass and heat lost in the atmosphere. Higher heating value (HHV) and lower heating value (LHV) are the parameters used to calculate the amount of hear from the biomass. HHV represents the heat required for the combustion per unit mass, while LHV is the subtraction of heat related to the vaporization of the existing water and water product from the heat required for combustion. The LHV for dry biomass is represented by,

$$LHV_{dry} = HHV_{dry} - 9Hq \tag{34}$$

where, H represents hydrogen content in dry biomass, which is 5%–7% and q is water condensation heat, equals to 2.4 MJ/kg. The variation between HHV and LHV is normally equal to 1–1.5 MJ/kg. Actual amount of LHV calculated from LHV_{dry} is as follows:

$$LHV = (1 - h)LHV_{dry} - hq = LHV_{dry} - h(LHV_{dry} - h(LHV_{dry} + q)) \tag{35}$$

where, h is moisture content on the wet basis.

In each ton of grain generally the ratio of dry matter at anthesis and final grin is among 1.29–1.50 t/ha. By taking an average of 1.4 ton/ha, the total amount of biomass available is 1,302,130.2 tons. Table 8 presented the standard biomass moisture contents.

The efficiency and capacity of power plant decrease as co firing ratio of biomass increases

$$\text{Efficiency Drop} = -0.4(co - fire\ ratio)^2 + 0.12(co - fire\ ratio)$$

$$P_e = P_{e.org} = \frac{\eta_{Biomass}}{\eta_{org}} \tag{36}$$

For calculating the biomass and coal needed in co-firing system is calculated as,

$$\frac{t.\text{biomass}}{\text{year}} = \text{Power Plant Size} * \%\text{Co} - \text{fire} * \text{Capacity Factor} * 8760\,{}^{\text{h}}/_{\text{yr}} * \text{Heat Rate} * [\text{HHV}]^{-1}_{\text{biomass}} \tag{37}$$

TABLE 8 Standard biomass moisture contents[36]

Matter	Mwb	Mdb
Bagasse	50%	100%
Barley straw	16%	19%
Corn stover	30%	42%
rice straw	67%	200%
Wheat straw	12%	14%
Forest residues	44%	78%
Primary mill residues	48%	91%
Urban wood residues	10%	14%

In this work, the capacity factor is selected as 80%. For normal operating conditions, the total biomass required by the power plant to generate 2.7 MW with co-firing capacity of 5%, heat rate 80% and HHV 80% is as follows:

$$\frac{\text{t.biomass}}{\text{year}} = 2700 * 0.05 * 0.8 * 8760\ {}^{\text{h}}/_{\text{yr}} * \frac{1}{0.8} = 1{,}182{,}600\ \text{t/year}$$

2.4 | Shunt capacitor modeling

To supply reactive power support, shunt capacitor (QGs) are used. The advantages of shunt capacitors are lower cost, improved voltage profile, and reduced losses. The maximum amount of capacitance value required can be calculated as follows[13,37]:

$$Q_{max} = U \times Q_o \tag{38}$$

where, U is an integer. In this work, U is taken as 9. Therefore, the required value of QG is 1.35 MVAr.

3 | METHODOLOGY AND PROBLEM FORMULATION

This section discusses the problem formulation for the optimal placement and sizing of the DGs and QGs resources used in this work by using MWOA.

3.1 | Optimal placement and sizing of DGs and QGs

The backward/forward load flow is used for performing the load flow analysis of the selected distribution network. In the process of optimization, active and reactive powers are injected from DG and QG, respectively based on the feeder current carrying capacity. It is less than the peak load, that is, sum of the power loss and power demand. In this work, to make the integration and compensation safe from the reverse current flow, it is taken as 80% of the total capacity limit as a network optimization constraint, while performing the system optimization for the radial distribution network using load flow. The ultimate goal of this work is to minimize the aggregate active power loss with minimized VD in the distribution network. This can be given as:

$$F_1 = min\left(\text{real}\left[\sum_{1}^{n} S_i\right]\right) \tag{39}$$

$$F_2 = min\sum_{i=1}^{m}(1 - V_i)^2 \tag{40}$$

where, $S_i = P + jQ$, n and m represent the number of branches and buses, respectively.

To optimize the above objective function under constraint conditions, the power flow equation should satisfy all the equality constraints presented below:

$$P_{sub} + P_{DG} = P_{loss} + P_{load} \tag{41}$$

$$Q_{sub} + Q_{shunt} = Q_{loss} + Q_{load} \tag{42}$$

where P_{sub} and $Q_{sub}$are the aggregate active and reactive power, injected by the sub-station into the network, P_{DG} and Q_{shunt} are the gross real and reactive power, injected by the DG and QG, respectively. P_{loss} and Q_{loss} are the aggregate active and reactive power losses in the network. P_{load} and Q_{load} are the gross active and reactive demands of the system.

The inequality constraints are as follows:
Voltage constraints are given by:

$$V_{min} \leq V_i \leq V_{max} \tag{43}$$

where, V_{min} is set to 0.95 and V_{max} is fixed to 1.05.

Feeder integrating capacity[17,18] is limited by its maximum thermal loading limit, that is,

$$I_{li} \leq I_{li,rated} \tag{44}$$

Location of DG (under the assumption that first bus is taken as slack bus)

$$2 \leq DG_{position} \leq n_{buses} \tag{45}$$

3.2 | Whale optimization algorithm (WOA)

WOA is the recent meta-heuristic algorithm developed by Mirjalili and Lewis[29] in the year 2016. The whales are highly intelligent animals. The special hunting behavior of the humpback whales inspired WOA, which prefer to hunt krill or small fishes, closer to the sea surface. Humpback whales special hunting called a bubble net-feeding method. For hunting, they swim around the prey and create distinct bubbles along a circle or nine-shaped path.[29]

From the basic characteristic of hunting, the following points are observed from the WOA.

3.2.1 | Encircling prey

One character of Whales predicts the current position is exact and in circles the prey. This character of social behavior is transformed in the mathematical equation, as the current best candidate solution set in the objective function. All other social groups will try updating their position status toward the best hunter. The behavior modeled is as:

$$\overrightarrow{X(t+1)} = \overrightarrow{X^*(t)} - \vec{A}.\vec{D} \tag{46}$$

$$\vec{D} = |\vec{C}.\overrightarrow{X^*}(t) - \vec{X}(t)| \tag{47}$$

$$\vec{A} = 2.\vec{a}.\vec{r} - \vec{a} \tag{48}$$

$$\vec{C} = 2.\vec{r} \tag{49}$$

where, $\overrightarrow{X^*}, \vec{X}$ represent the current position of best solution and position vector. Current iteration is denoted by t. $\vec{A}, \vec{C}$ are coefficient vectors. $\vec{a}$ is directly decreased from 2 to 0. $\vec{r}$ is a random vector [0,1].

3.2.2 | Bubble net-hunting method

In this hunting, character of whales, used two methods,

1. This time the whale encircles the prey and then shrinks from the far to the center: Here $\vec{A} \in [-a, a]$ where $\vec{A}$ is decreased from 2 to 0. Position $\vec{A}$ is setting down at random values between $[-1, 1]$. The new position $\vec{A}$ is computed between the previous position and the position of current best agent.

2. Spiral position updating: The whale shows a mimic helix-shaped movement to the prey, this property of whale can be represented in spiral equation:

$$\vec{X}(t+1) = \vec{D'}.e^{bl}.\cos(2\pi l) + \vec{X^*} \tag{50}$$

Prey may use more than two paths simultaneously, when whales hunt. In this work, 50% probability (*Prob*) is taken for the above two methods.

$$\vec{X}(t+1) = \begin{cases} \vec{X^*}(t) - \vec{A}.\vec{D}, & if\ Prob < 0.5 \\ \vec{D'}.e^{bl}.\cos(2\pi l) + \vec{X^*}, & if\ Prob \geq 0.5 \end{cases} \tag{51}$$

where, $D' = |\vec{X^*} - \vec{X}(t)|$ the distance between whale and the prey. b is the constant, $l \in [-1, 1]$. *Prob* is the arbitrary number from [0, 1]. Equation (49) presents the spiral-updating position.

3. To get the global possible optimum, updating has done with randomly

$$\vec{D} = |\vec{C}.\overrightarrow{X_{rand}} - \vec{X}| \tag{52}$$

$$\vec{X}(t+1) = \overrightarrow{X_{rand}} - \vec{A}.\vec{D} \tag{53}$$

$\overrightarrow{X_{rand}}$ is the random whale in current iteration.

3.3 | Implementation of MWOA

Here the MWOA is implemented using program algorithm with and without bound called by the same iteration and fitness limit. This implementation is presented in Figure 2 and performed as follows:

1. On the first sequence, the whales will be initialized first.
2. After initialization of whales, it is passed within the limits of DG/QG.
3. The numbers of iterations are performed.
4. On the second sequence, it will check with the same program beyond the limits of DG/QG.
5. Search the new fitness boundary.
6. Update positions using Equations (45) and (46).
7. Lastly, the value of optimization which is the most minimum loss will be recorded.

The algorithm utilized in this work is as follows[29]:
Step 1: Read 80% of the peak load of the feeder.
Step 2: Initialize the population.
Step 3: Generate the population of DG/QG sizes randomly using equation population = $(\mathrm{DG/QG_{max}} - \mathrm{DG/QG_{min}}) \times \mathrm{rand}\,() + \mathrm{DG/QG_{min}}$, where $\mathrm{DG/QG_{min}}$ and $\mathrm{DG/QG_{max}}$ are the minimum and maximum limits of DG/QG sizes.
Step 4: Solve the feeder-line flow.
Step 5: Find power losses for the generated population.
Step 6: If there is possible minimum power loss, search out of DG/QG limit, consider only the network limit.
Step 7: Set similar program out and call it to step 3.
Step 8: Current best solution DG and QG values with low losses.
Step 9: For updated population repeat step 6 and 7.
Step 10: If obtained losses are less, then replace current best solution with it or else go back to step 7.
Step 11: Record results if tolerance is <0.001 or go to step 2.
Step 12: By using Equations (46)–(53) update the position of whales.

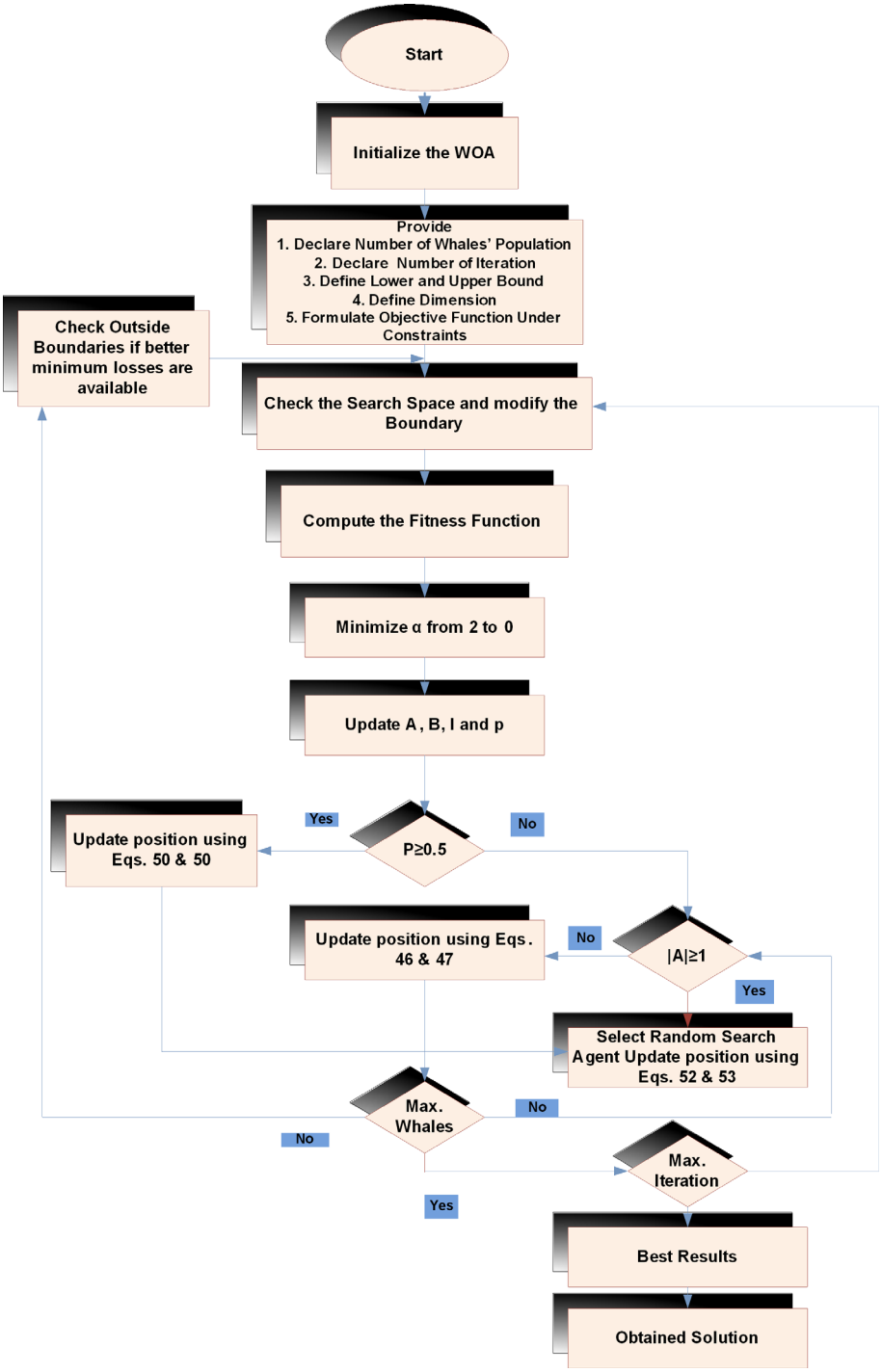

FIGURE 2 Flowchart of MWOA algorithm

4 | RESULTS AND COMPARATIVE ANALYSIS

This work performed on the Ghion and Bata feeder of the Bahir Dar distribution network. Bahir Dar substation-II has the 230/132/15 kV and 230/66/15 kV buses, which are power sources to four feeders (i.e., Air force, Bata, Ghion and Papyrus) and the other substation-I supply three feeders (i.e., Sematate, Boiler and Industry). For this study, two feeders, namely, Ghion and Bata are selected because the real power losses and voltage violations at these feeders are beyond the permissible limits. Figures 3 and 4 presented the single line diagrams of Ghion and Bata feeders, respectively. Further, Appendix Tables A1–A5 presented the various data, related to the modeling of the selected feeders.

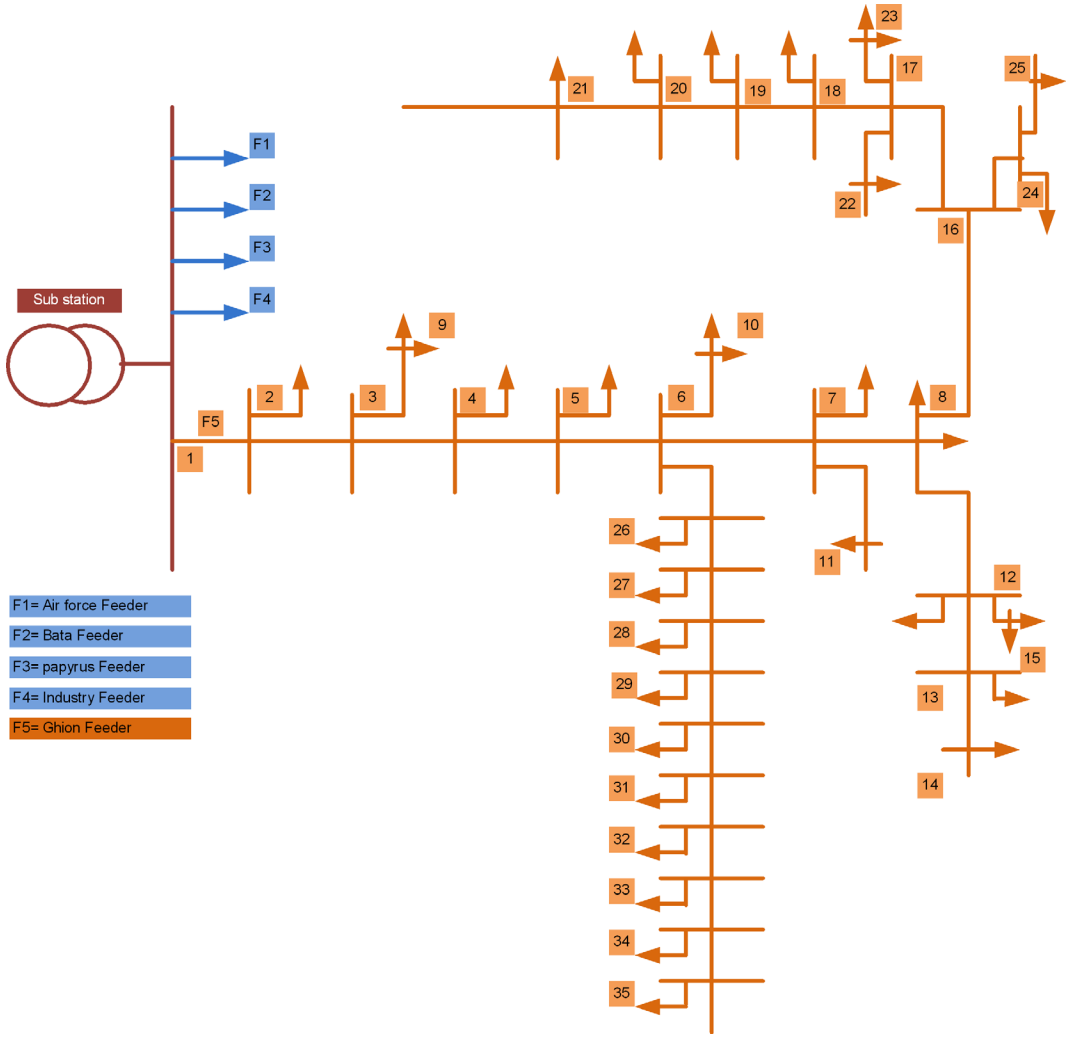

FIGURE 3 35-Bus Ghion feeder of Bahir Dar distribution system

Real power loss minimization by using integrating the active and reactive power source is applied to the two critical feeders of Bahir Dar radial distribution network. These feeders are connected from the Bahir Dar substation-II 400/230/66/15 kV bus. Feeder 5 is named as Ghion, which has 35 buses, while the other feeder named as Bata feeder has 40 buses.

Using the line and load data of the selected radial distribution network, backward/forward sweep load flow is performed to get the total feeder loss and initial voltage profile of the selected buses. In reasonable conditions, without any optimization, the total active load at the Bata feeder is 1.8262 MW with 1.5353 MVAr reactive loads. Ghion feeder has 3.43257 MW active and 2.5776 MVAr reactive loads. Additionally, the initial loss at the Bata feeder is 0.1262149 MW, and Ghion feeder is 0.3395703 MW.

In this work, for the system loss minimization, DG and QG sources are optimally sized and placed at the selected feeders by the MWOA optimization method. MWOA results are compared with the MPSO. The method is implemented using a MATLAB R2016 programming language with computer properties of 2.2 GHz processor and 7.58 GB RAM with core i7. The MATLAB program code is executed using the WOA algorithm. The proposed method minimized real power loss by optimizing the objective function under constraint conditions. For comparison, the parameters of the controlling values of MPSO are set as: the number of iterations is equal to 100, w is equal to 0.95, C_1 is equal to 2, C_2 is equal 2. In the case of MWOA, the iteration is the same as MPSO and the dimensions (dm) representing the total active power is set to one. The first bus is selected as the slack bus. The results are discussed in the following sub-sections.

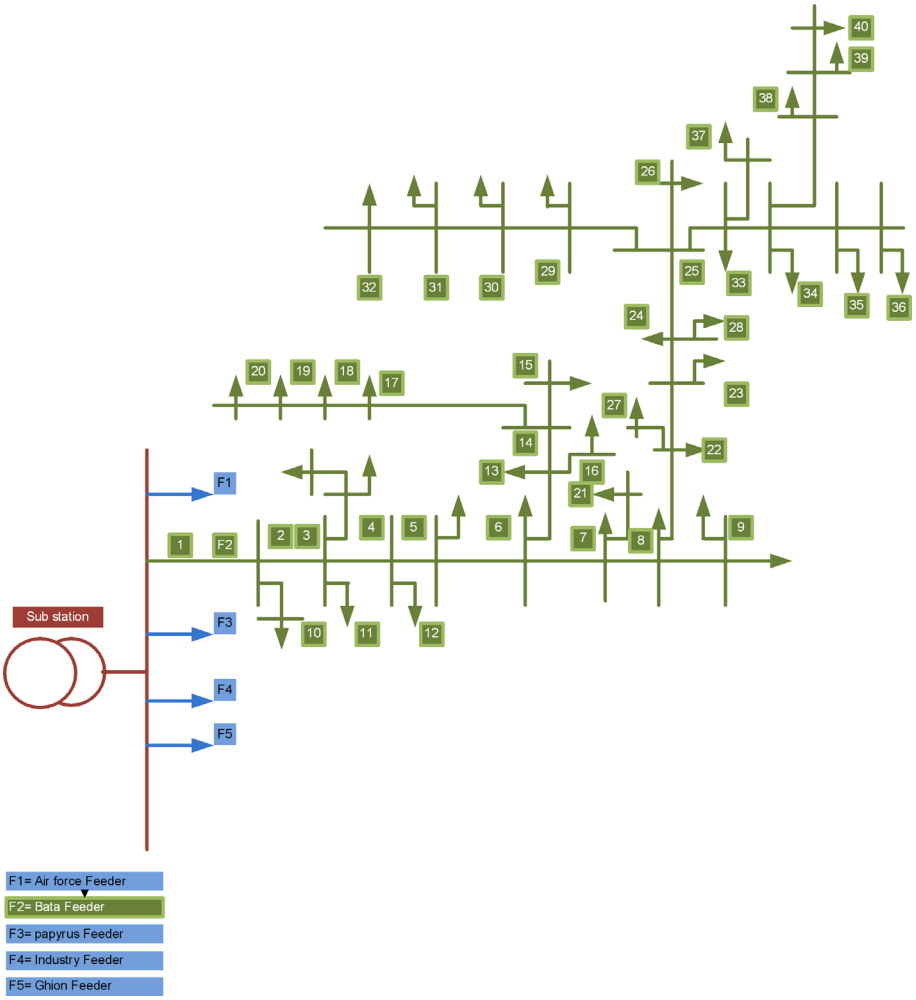

FIGURE 4 40-Bus Bata feeder of Bahir Dar distribution system

4.1 | Ghion feeder optimization

4.1.1 | Real power loss minimization

The result of the load flow provides the total real line losses as 339.5703 kW. When DG and QG are used as the source of optimization in the Ghion feeder, as seen from Table 9, the total active power loss after MWOA optimization is reduced to 22 kW. For comparative analysis, by implementing the MPSO optimization, the loss reduced to 27 kW. From the above result, the total power saved after the implementation of MWOA is 317.6 kW while with MPSO is 312.6 kW for Ghion feeder. Therefore, results concluded that MWOA provided better results compared to MPSO.

TABLE 9 Result summary of Ghion feeder buses

Method	P_{loss} (kW)	DG size	QG size	Location		V_{avg}
				DG	QG	
Load flow	339.5703	-	-	-	-	0.96
MPSO	27	3.16	1.709	28	27	0.988
MWOA	22	1.822	0.280	16	17	0.99

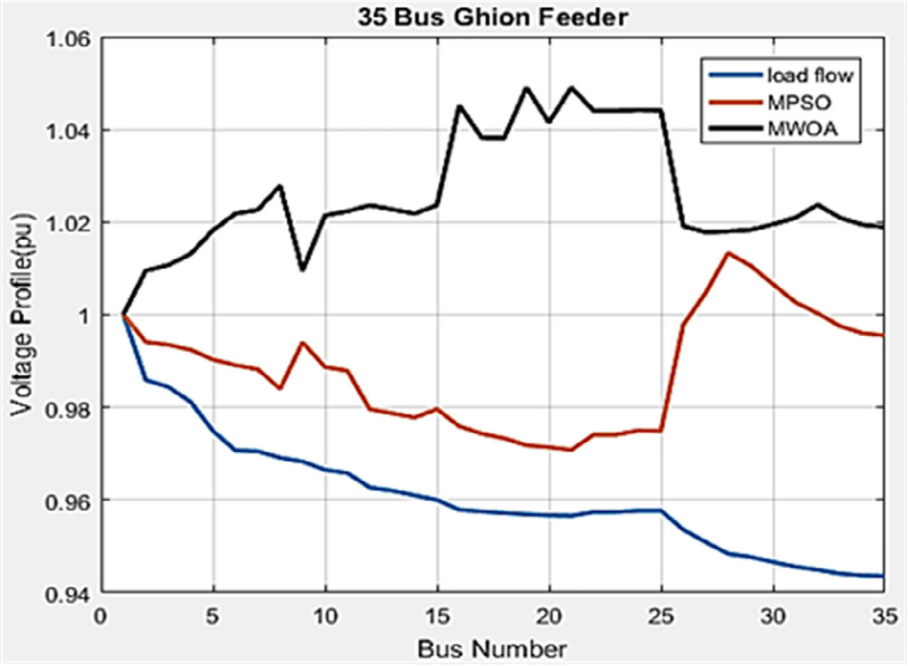

FIGURE 5 Voltage profile improvement of the 35-bus Ghion feeder before and after the optimization

4.1.2 | Voltage profile improvement

After the placement of DG and QG, the voltage profile is also upgraded. The load flow indicates that the average voltage profile of the feeder before the optimization is about 0.961 pu. The profile after the optimal sizing and placement of DG and QG by using MWOA is improved to 1.0258 pu while with MPSO is improved to 0.988 pu. The per branch profile of voltage after and before the optimization is shown in Figure 5.

The minimum value of voltages, before the placement of DG and QG are 0.9436 pu (at bus 35) and 0.9437 pu (at bus 34). With the MWOA optimization of the system, which is used for the placement and size of DG and QG, the value of voltages at the mentioned buses is improved to 1.0189 pu (at bus 35) and 1.0194 pu (at bus 34), while with the MPSO optimization, the values of voltages are improved to 0.9955 pu (at bus 35) and 0.9960 pu (at bus 34).

Figure 5 presented the comparative analysis of voltage profiles of Ghion feeder before and after the optimization performed using MWOA and MPSO.[30]

4.2 | Optimization of Bata feeder

4.2.1 | Real power loss minimization

The result of the load flow provides the total real line losses as 126.2149 kW. In the optimization process of the 40-bus Bata feeder by optimally integrating DG and QG, as seen from Table 10, the aggregated active power loss calculated by MWOA is reduced to 22.4 kW while with MPSO reduced to 51.3 kW. From the results, the total power saved after MWOA optimization is 103.814 kW while with MPSO is 74.914 kW.

4.2.2 | Voltage profile improvement of Bata feeder

After the optimal placement of DG and QG, the voltage profile of various buses the Bata feeder is improved. The average voltage profile of the feeder before the optimization is 0.9727 pu. The voltage profile after optimally placing the DG and QG with the help of MWOA is improved to 0.9991 pu while with MPSO, it is improved to 0.9890 pu. Figure 6 presented the comparative analysis of voltage profiles of Bata feeder before and after the optimization, performed by MWOA and MPSO.

TABLE 10 Result summary of Bata feeder buses

Method	P_{loss} (kW)	DG size	QG size	Location		V_{avg}
				DG	QG	
Load flow	126.215	-	-	-	-	0.9727
MPSO	51.3	1.437	1.1434	25	24	0.989
MWOA	22.4	0.820	1.070	35	31	0.999

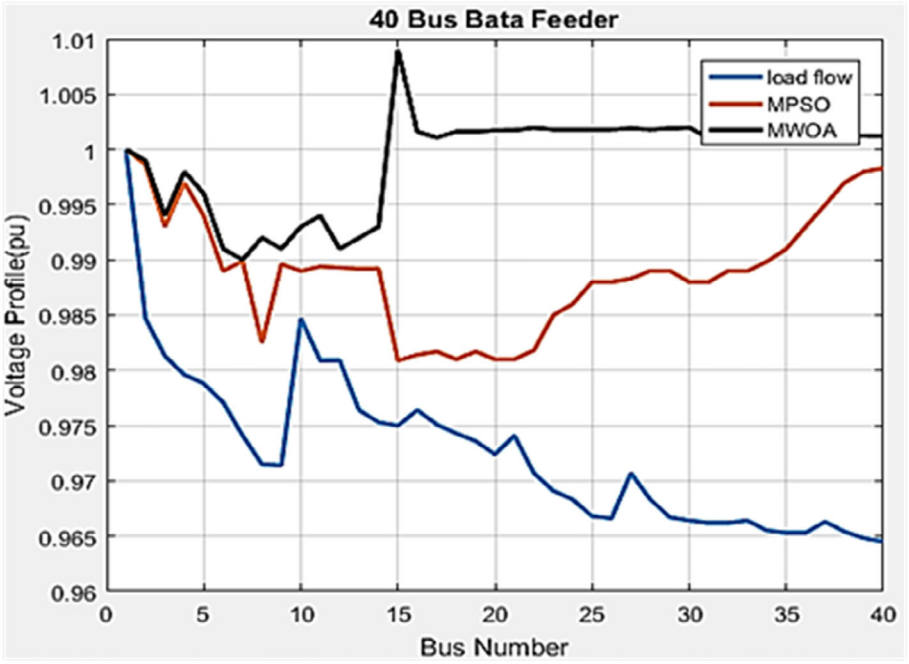

FIGURE 6 Voltage profile improvement of the 40-bus Bata feeder before and after the optimization

4.3 | Performance comparison study of existing system with MWOA and MPSO

This work optimizes the real power loss minimization problem by satisfying all the constraints. The active power loss is reduced, and the voltage profiles are improved. It is often robust to consider feeder voltage regulation related to the profiles of feeder voltage. Voltage profile indicates the magnitude of the voltage with respect to its location on the feeder. One way to determine the quality of power is maintaining the receiving end voltage magnitude closer the same to the sender end. For bring this achievement practically, the capacitor and DG are applied in this work for Bahir Dar distribution system. The size and placement of DG and shunt capacitor are performed by MWOA which illustrated using the 35-bus Ghion feeder and 40-bus Bata feeder, the practical feeders of the Bhir Dar distribution system. The real power losses, DG and QG sizes with location and average voltage profile of these feeders before and after the optimization is presented in Tables 9 and 10.

Optimal location and size of DG and QG are found with the help of MWOA and compared with MPSO. After optimization, the power loss had reduced from 339.5703 to 22 kW in Ghion feeder and from 126.2149 to 22.4 kW in Bata feeder using MWOA. It had reduced from 339.5703 to 27 kW in Ghion feeder and from 126.2149 to 51.3 kW in Bata feeder using MPSO.

The algorithm developed for the power loss reduction by applying shunt compensation of capacitor and DG integration had improved the overall system voltage profile. As a result, the voltage profile before the optimization is 0.96, after optimization with MPSO, it is improved to 0.988 pu, and after optimization with MWOA, it is improved to 0.997 pu for Ghion feeder. The voltage profile of Bata feeder before and after optimization is 0.9726. After optimization with the MPSO is improved to 0.989 and with MWOA improved to 0.9991 pu in Bata feeder. From the results, MWOA provided better performance as compare to the MPSO optimization approach.

TABLE 11 Expected cost of DG and QG in USD/W and kVAr

Technology	Investment cost ($/W)	Capacitor cost ($/kVAr)
Biomass	1.5–2.5	5
Wind	0.8–1.5	
Solar PV	6–8	

TABLE 12 Total investment cost

Technology	Size	Investment cost ($)
Biomass	2.7 (MW)	4,050,000–10,125,000
Wind	2.41 (MW)	1,928,000–2,892,000
Solar, PV	0.29 (MW)	1,740,000–13,920,000
QG	1.35 (MVAr)	6750
Total investment cost		7,724,750–26,943,750
Average of total investment cost		17,334,250

4.4 | Power output from various sources

The wind power density and the capacity factor of Bahir Dar are very suitable for wind generation. Hence, two wind turbines are considered in this study to supply the main power demand. Rest demand which is not covered by the wind generation is supplied by solar power. The output of Vestas V82 wind turbine at average speed of 10.43 m/s is 1210 kW. Therefore, the total generation from two wind turbines is 2410 kW.

The required solar power is (2700–2410 kW) 290 kW. The daily average solar radiation of Bahir Dar city is 6.286 kWh/m^2/d. The solar irradiance computed for the Bahir Dar city is 1322.73 W/m^2. The solar power output at 1322.73 W/m^2 is about 190 W with this output about 1527 solar panels are required.

Biomass resource is utilized as the backup source in this work. To minimize the investment cost of the biomass, it should be installed at 16th bus of Ghion feeder and 35th bus of Bata feeder. The total DG value calculated from MWOA optimization is about 2.7 MW. Since biomass is utilized as back up, its value should equal to the total power demanded from DG, that is, 2.7 MW. For normal operating conditions, the total biomass required by the power plant to generate 2.7 MW with co-firing capacity of 5%, heat rate 80% and HHV 80% are 1,182,600 tons/year.

The QG value of the two feeders after WOA optimization is 1.35 MVAr. The value of QG can be found in multiple of 150 kVAr.

4.5 | Investment cost of overall system

For the development of wind, solar and biomass power plant based DG system, the investment cost and shunt capacitor cost is summarized in Table 11[31,34]:

The investment cost of the system, optimized using WOA for the selected two feeders is presented in Table 12. Since wind capacity factor is higher, it is reasonable to choose two wind turbines and the rest should be solar energy. The biomass is used as backup source to avoid intermittence nature of wind and solar energy. Hence, it would cover all the power supplied by solar and wind during their off condition. Further, shunt capacitor is used to supply reactive power, required by the system.

5 | CONCLUSION

Localizing the active generation and reactive power demands had reduced the power loss. In this research, multi-objective-based WOA optimization is applied to minimize the practical system losses. In this work, two practical feeders of the Bahir Dar distribution network was considered to perform the loss minimization as well as voltage profile improvement. MWOA was compared with the MPSO, which shows the superiority of the initial one in terms of loss minimization and voltage profile improvement. A detailed economic analysis is also presented, which shows the total investment cost

required for the DG and capacitor bank installation. As the future enhancement of this work, maximum loading condition of the selected feeders can be incorporated to show the performance of the optimization techniques at peak loading. Further, in whole Bahir Dar distribution network can be considered under different constraints conditions of the power system for the better understanding of the system performance. Further, other machine learning based optimization techniques can be utilized in real time manner for dynamic operation optimization of the system. The proposed work can also be applied to other types of the multi-energy networks.[38]

ACKNOWLEDGMENTS

This work was supported by VILLUM FONDEN under the VILLUM Investigator Grant (no. 25920): Center for Research on Microgrids (CROM); www.crom.et.aau.dk.

PEER REVIEW

The peer review history for this article is available at https://publons.com/publon/10.1002/eng2.12455.

DATA AVAILABILITY STATEMENT

Research data are not shared.

CONFLICT OF INTEREST

The authors declare no potential conflict of interest.

AUTHOR CONTRIBUTIONS

Bawoke Simachew: Conceptualization (equal); data curation (equal); formal analysis (equal); investigation (equal); methodology (equal); project administration (equal); resources (equal); software (equal); visualization (equal); writing – original draft (equal); writing – review and editing (equal). **Baseem Khan:** Conceptualization (equal); data curation (equal); formal analysis (equal); investigation (equal); methodology (equal); project administration (equal); resources (equal); software (equal); supervision (equal); validation (equal); visualization (equal); writing – original draft (equal); writing – review and editing (equal). **Josep M Guerrero:** Supervision (equal); validation (equal). **Sanjeevikumar Padmanaban:** Supervision (equal); visualization (equal). **Om Prakash Mahela:** Visualization (equal); writing – review and editing (equal). **Hassan Haes Alhelou:** Visualization (equal); writing – review and editing (equal).

ORCID

Baseem Khan https://orcid.org/0000-0002-5082-8311
Josep M. Guerrero https://orcid.org/0000-0001-5236-4592

REFERENCES

1. Short T, Swayne T. *Assessment of Transmission and Distribution Losses in New York PID071178 (NYSERDA 15464)*. The New York State Energy Research and Development Authority; 2012.
2. Badran O, Mekhilef S, Mokhlis H, Dahalan W. Optimal reconfiguration of distribution system connected with distributed generations: a review of different methodologies. *Renew Sustain Energy Rev*. 2017;73:854-867.
3. Tostado-Véliz M, Matos MA, Peças Lopes JA, Jurado F. An improved version of the continuous Newton's method for efficiently solving the power-flow in ill-conditioned systems. *Int J Electr Power Energy Syst*. 2021;124:106389.
4. Tostado-Véliz M, Kamel S, Jurado F. Power flow approach based on the S-iteration process. *IEEE Trans Power Syst*. 2020;35(6):4148-4158.
5. Ali A, Nor NM, Ibrahim T, Romlie MF. Sizing and placement of battery-coupled distributed photovoltaic generations. *J Renew Sustain Energy*. 2017;9(5).
6. Padma Lalitha M, Suresh Babu P, Adivesh B. Optimal distributed generation and capacitor placement for loss minimization and voltage profile improvement using symbiotic organisms search algorithm. *Int J Electr Eng*. 2016;9(3):250-262.
7. Abdelaziz AY, Ali ES, Abd Elazim SM. Optimal sizing and locations of capacitors in radial distribution systems via flower pollination optimization algorithm and power loss index. *Eng Sci Technol*. 2016;19(1):610-618.
8. Reddy PDP, Reddy VCV, Manohar TG. Whale optimization algorithm for optimal sizing of renewable resources for loss reduction in distribution systems. *Renew Wind Water Solar*. 2017;4(3):1-13.
9. Wang C, Yao G, Wang X, et al. Reactive power optimization based on particle swarm optimization algorithm in 10 kV distribution network. In: Tan Y, Shi Y, Chai Y, Wang G, eds. *Advances in Swarm Intelligence. ICSI 2011*. Lecture Notes in Computer Science. Vol 6728. Springer; 2011.
10. Bhullar S, Ghosh S. Optimal integration of multi distributed generation sources in radial distribution networks using a hybrid algorithm. *Energies*. 2018;12(4–5):2-15.

11. Xie J, Liang C, Xiao Y. Reactive power optimization for distribution network based on distributed random gradient-free algorithm. *Energies*. 2018;11:534.
12. Boktor CG, Youssef AR, Ali AH, Kamel S. Optimal distribution power flow including shunt capacitor allocation based on voltage deviation and power loss minimization. Proceedings at the 2017 Nineteenth International Middle East Power Systems Conference (MEPCON); 2017: Menoufia University.
13. Elsheikh A, Helmy Y, Abouelseoud Y, Elsherif A. Optimal capacitor placement and sizing in radial electric power systems. *Alex Eng J*. 2014;53(4):809-816.
14. Thang VV, Minh ND. Optimal allocation and sizing of capacitors for distribution systems reinforcement based on minimum life cycle cost and considering uncertainties. *Open Electr Electron Eng J*. 2017;11(18):165-176.
15. Hassanzadeh Fard H, Jalilian A. Optimal sizing and location of renewable energy based DG units in distribution systems considering load growth. *Int J Electr Power Energy Syst*. 2018;101:356-370.
16. Prakash DB, Lakshminarayana C. Optimal siting of capacitors in radial distribution network using whale optimization algorithm. *Alex Eng J*. 2017;56(4):499-509.
17. Kumar M, Nallagownden P, Elamvazuthi I. Optimal placement and sizing of renewable distributed generations and capacitor banks into radial distribution systems. *Energies*. 2017;10:811 [15].
18. Kumar M, Nallagownden P, Elamvazuthi I. Multi-objective PSO based optimal placement of solar power DG in radial distribution system. *J Electr Syst*. 2017;13(2):322-331.
19. Shehata RH, Mekhamer SF, Abdelaziz AY, Badr MAL. Solution of the capacitor allocation problem using an improved whale optimization algorithm. *Int J Eng Sci Technol*. 2018;10(4):1-11.
20. Ang S, Leeton U, Kulworawanichpong T, Chayakulkeeree K. Multi-objective real power loss and voltage deviation minimization for grid connected micro power system using whale optimization algorithm. *Int Energy J*. 2018;18:297-310.
21. Essam A, Al-Ammar KF, Waqar A, et al. ABC algorithm based optimal sizing and placement of DGs in distribution networks considering multiple objectives. *Ain Shams Eng J*. 2021;12(1):697-708.
22. Roy NB, Das D. Optimal allocation of active and reactive power of dispatchable distributed generators in a droop controlled islanded microgrid considering renewable generation and load demand uncertainties. *Sustain Energy Grids Netw*. 2021;27.
23. Ziad M, Ali IMD, El-Rafei A, Hasanien HM, Abdel Aleem SHE, Abdelaziz AY. A novel distributed generation planning algorithm via graphically-based network reconfiguration and soft open points placement using Archimedes optimization algorithm. *Ain Shams Eng J*. 2021;12(2):1923-1941.
24. Öner A, Abur A. Voltage stability based placement of distributed generation against extreme events. *Electr Power Syst Res*. 2020;189:106713.
25. Rafi V, Dhal PK. Maximization of economy in distribution networks with most favorable placement of distributed generators along with reorganization using hybrid optimization algorithm. *Mater Today: Proc*. 2020;33(7):4094-4100.
26. Ahmadi M, Adewuyi OB, Danish MSS, Mandal P, Yona A, Senjyu T. Optimum coordination of centralized and distributed renewable power generation incorporating battery storage system into the electric distribution network. *Int J Electr Power Energy Syst*. 2021;125.
27. Tolabi HB, Lashkar Ara A, Hosseini R. A new thief and police algorithm and its application in simultaneous reconfiguration with optimal allocation of capacitor and distributed generation units. *Energy*. 2020;203:117911.
28. Routray A, Mistry KD, Arya SR. Wake analysis on wind farm power generation for loss minimization in radial distribution system. *Renew Energy Focus*. 2020;34:99-108.
29. Mirjalili S, Lewis A. The whale optimization algorithm. *Adv Eng Softw*. 2016;95:51-67.
30. Kennedy J, Eberhart R. Particle swarm optimization. Proceedings of ICNN'95 – International Conference on Neural Networks; 1995, 4:1942–1948.
31. Patel MR. *Wind and Solar Power Systems Design, Analysis, and Operation*. CRC Press; 2006.
32. Javed MS, Song A, Ma T. Techno-economic assessment of a stand-alone hybrid solar-wind-battery system for a remote Island using genetic algorithm. *Energy*. 2019;176:704-717.
33. Sampaio PGV, González MOA. Photovoltaic solar energy: conceptual framework. *Renew Sustain Energy Revi*. 2017;74:590-601.
34. "Solar Power System," Free Energy Planet; 2017. [Online]. Accessed 28 May, 2020. https://www.freeenergyplanet.biz/solar-power-systems/solar-photovoltaic-power-system-1.html.
35. Chanie Y, Teshome A, Temesgen Y, Berihun B. Characterization of potato production, marketing, and utilization in North Western Amhara region, Ethiopia. *J Horticulture Forestry*. 2017;9(3):17-25.
36. Jennie Jorgenson PG. *Technical Manual for the SAM Biomass Power Generation Model*. Colorado: National Renewable Energy Laboratory; 2011. https://www.nrel.gov/docs/fy11osti/52688.pdf. Accessed 23 August, 2020.
37. Soleymani S, Mozafari B, Kamarposhti MA. Optimal capacitor placement for power loss reduction and voltage stability enhancement in distribution systems. *Trakia J Sci*. 2014;12:425-430.
38. Tostado-Véliz M, Arévalo P, Jurado F. A comprehensive electrical-gas-hydrogen microgrid model for energy management applications. *Energy Convers Manag*. 2021;228:113726.

How to cite this article: Simachew B, Khan B, Guerrero JM, Padmanaban S, Mahela OP, Alhelou HH. Capacity-based optimization using whale optimization technique of a power distribution network. *Engineering Reports*. 2022;4(1):e12455. doi: 10.1002/eng2.12455

APPENDIX A

TABLE A1 Power flow results of Bata feeder

Bus no	Active power flow before optimization (kW)	Reactive power flow before optimization (kVAr)
1	0	0
2	9.96	6.69
3	59.34	62.26
4	15.77	10.59
5	0	0
6	0	0
7	0	0
8	38	28.5
9	146.76	124.08
10	71.71	71.11
11	136.74	103.84
12	0	0
13	0	0
14	53.39	44.65
15	65.45	54.22
16	70.4	52.8
17	31.98	21.8
18	78.28	66.93
19	40.8	30.6
20	159.75	158.43
21	0	0
22	75.07	62.2
23	0	0
24	0	0
25	17.22	12.02
26	113	96.82
27	45.6	38.99
28	18.04	12.59
29	45.81	37.96
30	64.6	55.23
31	36.52	24.54
32	18.4	13.8
33	8.3	5.58
34	24.45	17.37
35	57.75	48.74
36	12.3	8.58
37	68.5	47.8
38	88	66
39	93.5	86
40	94.6	88

TABLE A2 Load flow results in per unit of the Bata feeder before and after optimization

Bus No	Vbus (pu) before optimization	Vbus (pu) after PSO optimization	Vbus (pu) after WOA optimization
1	1	1	1
2	0.9847	0.9986	1.0402
3	0.9813	0.9843	1.014
4	0.9796	0.9837	1.0176
5	0.9788	0.9834	1.0212
6	0.9771	0.9827	0.9991
7	0.9741	0.9886	1.032
8	0.9715	0.9889	1.0108
9	0.9714	0.9886	1.0391
10	0.9847	0.9862	1.0469
11	0.9809	0.9812	1.007
12	0.9809	0.9812	1.0401
13	0.9764	0.9758	1.0182
14	0.9753	0.9721	1.0454
15	0.975	0.9709	1.0089
16	0.9764	0.9754	1.0217
17	0.9751	0.9797	1.0188
18	0.9743	0.9771	1
19	0.9736	0.9747	1.0321
20	0.9724	0.9705	1.0022
21	0.9741	0.986	1.0253
22	0.9707	0.9937	1.0096
23	0.9691	0.9985	1.0014
24	0.9683	1.001	1.0195
25	0.9668	1.0058	0.9974
26	0.9666	1.0051	1.0381
27	0.9707	0.9933	1.0164
28	0.9683	1.0009	0.9987
29	0.9667	1.0057	0.9999
30	0.9664	1.0061	1.0447
31	0.9662	1.0077	1.0206
32	0.9662	1.0076	1.0334
33	0.9664	1.0017	1.0275
34	0.9655	0.9984	1.0258
35	0.9653	0.9981	1.0256
36	0.9653	0.998	1.0255
37	0.9663	1.001	1.0271
38	0.9654	0.9977	1.0254
39	0.9648	0.9981	1.0242
40	0.9645	0.9983	1.0232

TABLE A3 Load flow results in per unit of the Ghion feeder before and after optimization

Bus number	Vbus (pu) before optimization	Vbus (pu) after PSO optimization	Vbus (pu) after WOA optimization
1	1	1	1
2	0.9859	0.9941	1.0095
3	0.9844	0.9935	1.0107
4	0.9812	0.9924	1.0131
5	0.9749	0.9903	1.0182
6	0.9707	0.9891	1.0218
7	0.9705	0.9882	1.0226
8	0.9691	0.984	1.0278
9	0.9683	0.994	1.0095
10	0.9665	0.9887	1.0214
11	0.9658	0.9879	1.0223
12	0.9627	0.9796	1.0236
13	0.962	0.9787	1.0227
14	0.961	0.9778	1.0218
15	0.96	0.9796	1.0236
16	0.9579	0.9759	1.0451
17	0.9575	0.9743	1.0382
18	0.9572	0.9733	1.0381
19	0.9569	0.9718	1.049
20	0.9567	0.9714	1.0415
21	0.9566	0.9708	1.049
22	0.9574	0.9741	1.044
23	0.9574	0.9741	1.044
24	0.9577	0.975	1.0442
25	0.9577	0.9749	1.0441
26	0.9536	0.9978	1.0191
27	0.9509	1.0047	1.0178
28	0.9484	1.0133	1.018
29	0.9477	1.0106	1.0183
30	0.9466	1.0066	1.0195
31	0.9456	1.0027	1.0209
32	0.9449	1.0003	1.0237
33	0.9441	0.9975	1.0209
34	0.9437	0.996	1.0194
35	0.9436	0.9955	1.0189

TABLE A4 Bus and line data of 30 bus Ghion feeder of Bahir Dar distribution system

Sending End	Receiving End	Conductor Type	Length in km	Resistance(Ω)	Reactance in (Ω)	Receiving end load (kW)	Receiving end load (kVAr)
1	2	AAC-95	1.687	0.5760	0.0845	0	0
2	3	AAC-95	0.209	0.0645	0.0095	25.60	19.20
3	4	AAC-95	0.423	0.1305	0.0191	11.62	7.80
4	5	AAC-95	0.857	0.2644	0.0388	17.62	32.90
5	6	AAC-95	0.577	0.1780	0.0261	47.15	0
6	7	AAC-95	0.085	0.0262	0.0038	0	0
7	8	AAC-95	0.457	0.1410	0.0207	0	222.30
2	9	AAC-50	0.191	0.1105	0.0130	260	20.88
6	10	AAC-50	0.430	0.2488	0.0292	29.93	28.32
7	11	AAC-50	0.170	0.0983	0.0115	68.0	51.00
8	12	AAC-50	0.897	0.5189	0.0609	130.8	88.68
12	13	AAC-50	0.229	0.1325	0.0155	43.20	32.40
13	14	AAC-50	0.334	0.1932	0.0227	108.3	72.26
12	15	AAC-50	0.474	0.2742	0.0322	164.92	141.01
8	16	AAC-50	0.944	0.5461	0.0641	0	0
16	17	AAC-50	0.221	0.1278	0.0150	0	0
17	18	AAC-50	0.204	0.1180	0.0138	51.48	44.02
18	19	AAC-50	0.345	0.1996	0.0234	55.82	46.25
19	20	AAC-50	0.174	0.1007	0.0118	92.78	76.87
20	21	AAC-50	0.344	0.1990	0.0234	73.61	60.98
17	22	AAC-50	0.180	0.1041	0.0122	99.30	79.12
17	23	AAC-50	0.399	0.2308	0.0271	69.81	51.73
16	24	AAC-50	0.791	0.4576	0.0537	33.62	23.46
24	25	AAC-50	0.179	0.1036	0.0122	17.01	11.43
6	26	AAC-50	0.2184	0.2999	0.0352	60	20
26	27	AAC-50	0.268	0.2129	0.0250	120	70
27	28	AAC-50	0.184	0.2221	0.0261	200	600
28	29	AAC-50	0.22	0.0706	0.0083	150	70
29	30	AAC-50	0.338	0.1237	0.0145	210	100
30	31	AAC-50	0.168	0.1254	0.0147	60	40
31	32	AAC-50	0.26	0.1250	0.0147	460	250
32	33	AAC-50	0.184	0.2221	0.0261	256	120
33	34	AAC-50	0.228	0.1319	0.0155	36	15
34	35	AAC-50	0.388	0.1435	0.0168	342	122
						138	60

TABLE A5 Bus and line data of 40 bus Bata feeder of Bahir Dar distribution system

Sending end	Receiving end	Conductor type	Length in km	Resistance (Ω)	Reactance in (Ω)	Receiving end load (kW)	Receiving end load (kVAr)
1	2	AAC-95	1.784	0.550364	0.081071974	0	0
2	3	AAC-95	0.427	0.13173	0.019404559	9.96	6.69
3	4	AAC-95	0.229	0.070647	0.01040666	59.34	62.26
4	5	AAC-95	0.114	0.035169	0.005180608	15.77	10.59
5	6	AAC-95	0.236	0.072806	0.010724768	0	0
6	7	AAC-95	0.621	0.191579	0.028220682	0	0
7	8	AAC-95	0.543	0.167516	0.024676055	0	0
8	9	AAC-95	0.143	0.044116	0.006498482	38	28.5
2	10	AAC-50	0.336	0.194376	0.022874473	146.76	124.08
3	11	AAC-50	0.833	0.481891	0.056709632	71.71	71.11
11	12	AAC-50	0.894	0.517179	0.060862438	136.74	103.84
6	13	AAC-50	0.481	0.278259	0.032745898	0	0
13	14	AAC-50	0.297	0.171815	0.020219401	0	0
14	15	AAC-50	0.65	0.376025	0.044251213	53.39	44.65
13	16	AAC-50	0.211	0.122064	0.014364625	65.45	54.22
14	17	AAC-50	0.268	0.155038	0.018245116	70.40	52.8
17	18	AAC-50	0.324	0.187434	0.022057528	31.98	21.8
18	19	AAC-50	0.402	0.232557	0.027367673	78.28	66.93
19	20	AAC-50	0.893	0.516601	0.060794359	40.8	30.6
7	21	AAC-50	0.314	0.181649	0.02137674	159.75	158.43
8	22	AAC-50	0.326	0.188591	0.022193685	0	0
22	23	AAC-50	0.264	0.152724	0.0179728	75.07	62.2
23	24	AAC-50	0.134	0.077519	0.009122558	0	0
24	25	AAC-50	0.25	0.144625	0.017019697	0	0
25	26	AAC-50	0.21	0.121485	0.014296546	17.22	12.02
22	27	AAC-50	0.314	0.181649	0.02137674	113	96.82
24	28	AAC-50	0.188	0.108758	0.012798812	45.6	38.99
25	29	AAC-50	0.121	0.069999	0.008237534	18.04	12.59
29	30	AAC-50	0.275	0.159088	0.018721667	45.81	37.96
30	31	AAC-50	0.43	0.248755	0.02927388	64.6	55.23
31	32	AAC-50	0.33	0.190905	0.022466001	36.52	24.54
25	33	AAC-50	0.328	0.189748	0.022329843	18.4	13.8
33	34	AAC-50	0.318	0.183963	0.021649055	8.3	5.58
34	35	AAC-50	0.197	0.113965	0.013411522	24.45	17.37
35	36	AAC-50	0.242	0.139997	0.016475067	57.75	48.74
33	37	AAC-50	0.379	0.219252	0.025801861	12.3	8.58
34	38	AAC-50	0.091	0.052644	0.00619517	68.5	47.8
38	39	AAC-50	0.418	0.241813	0.028456934	88	66
39	40	AAC-50	0.727	0.42057	0.04949328	93.5	86
						94.6	88.0